Determination of the interaction parameter and topological scaling features of symmetric star polymers in dilute solution

Durgesh K. Rai, Gregory Beaucage, Kedar Ratkanthwar, Peter Beaucage, Ramnath Ramachandran, and Nikos Hadjichristidis

Phys. Rev. E **92**, 012602 — Published 15 July 2015

DOI: 10.1103/PhysRevE.92.012602

Determination of the interaction parameter and topological scaling features of symmetric star polymers in dilute solution

Durgesh K Rai[1], Gregory Beaucage[2*], Kedar Ratkanthwar[3,4], Peter Beaucage[5], Ramanath Ramachandran[6], Nikos Hadjichristidis[3,4]

[1]Oak Ridge National Laboratory, [2]University of Cincinnati, [3]University of Athens, [4]King Abdullah University of Science and Technology, [5]Cornell University, [6]Procter & Gamble

Abstract

Star polymers provide model architectures to understand the dynamic and rheological effects of chain confinement for a range of complex topological structures like branched polymers, colloids and micelles. It is important to describe the structure of such macromolecular topologies using small-angle neutron and x-ray scattering to facilitate understanding of their structure-property relationships. Modeling of scattering from linear, Gaussian polymers, such as in the melt, has applied the random phase approximation (RPA) using the Debye polymer scattering function. The Flory-Huggins interaction parameter can be obtained using neutron scattering by this method. Gaussian scaling no longer applies for more complicated chain topologies or when chains are in good solvents. For symmetric star polymers, chain scaling can differ from $\nu = 0.5$ ($d_f = 2$) due to excluded volume, steric interaction between arms, and enhanced density due to branching. Further, correlations between arms in a symmetric star leads to an interference term in the scattering function first described by Benoit for Gaussian chains. In this work, a scattering function is derived which accounts for inter-arm correlations in symmetric star polymers as well as the polymer-solvent interaction parameter for chains of arbitrary scaling dimension using a hybrid Unified scattering function. The approach is demonstrated for linear, 4-arm and 8-arm polyisoprene stars in deuterated *p*-xylene.

[*]Corresponding Author. E-mail: beaucag@uc.edu, gbeaucage@gmail.com

Introduction

Symmetric star polymers provide an ideal architecture to examine chain interactions in macromolecules [1-9]. The presence of a branch point leads to topology driven rearrangements of individual arms in dilute solutions and therefore the thermodynamic and structural characteristics differ from their linear counterparts [1, 3, 6, 10-20]. The interaction of arms affect the molecular conformation affecting rheological properties, which have been found ideally suitable for drug delivery, polymer electrolytes in lithium batteries, additives to improve water flooding during enhanced oil recovery process of fracking and other applications [2, 9, 13, 21-31].

Small-angle x-ray and neutron scattering from star polymers is often fit using the Benoit function for symmetric stars [32-34]. The Benoit function assumes Gaussian scaling. The function accounts for correlations between the arms through the addition of a correlation term to the Debye function, equation (1).

$$I(q) = \frac{2G}{Q^2}\left(e^{-Q} - 1 + Q\right) \tag{1}$$

where $Q = q^2 R_g^2$, q is the scattering vector, G is the scattered intensity at $q \to 0$, and R_g is the Gaussian coil radius of gyration [35]. To extend the Benoit approach to non-Gaussian conditions, an empirical function was proposed by Dozier based on the work of Teixeira and Sinha [13, 25, 36] that has had limited success in parameterizing scattering from symmetric stars in the presence of excluded volume. The Dozier function is not based on a structural model and is an *ad hoc* function, so it is unlikely to result in valid structural information.

In dilute solution equation (1) is generally not applicable since chains generally display exclude volume altering the structural scaling coefficient $v = 1/d_f$, where d_f is the

mass fractal dimension for the coil. For equation (1), $d_f = 2$. In good solvents, for a linear chain, $d_f = 5/3$ due to excluded volume. For chains with complex structures, such as branched chains, cyclics and networked chains, d_f is known to increase due to the increase in topological complexity [37]. In crowded conditions, such as in high functionality star polymers with functionality $f >> 3$, the arms of the polymer have correlations that cannot be ignored especially at high *f*.

At high *f,* $f >> 8$, these correlations transform the fractal structure to colloidal particles [13] as described by the Daoud-Cotton model [10]. For example, Likos *et al.* [20] discuss star polymers that display a "core" and a polymeric shell similar to the Daoud-Cotton model [10] for star polymers with $f = 18$. The arm length, the solvent quality, the functionality, charge, and hydrophilicity of the arms govern the transition to from fractal/polymeric to colloidal Daoud Cotton structures. Therefore it is probably necessary to consider more than just star functionality.

Equation (1) has the further limitation that it ignores the effect of enthalpic interactions between the polymer's zero conformational entropy Kuhn unit and the solvent (or polymer in a blend). The presence of attractive enthalpic interactions leads to a diminution of the scattered intensity at low angles that has been modeled using an analogy to screening in charged colloids [20]. At sizes larger than the screening length the system appears to be uniform since concentration fluctuations dominate the scattering compared to the chain form factor of equation (1). This effect was first modeled using a double extrapolation to zero scattering angle and to zero concentration in the Zimm plot [1]. The modified Zimm approach of Stein and Hadziioannou [38], later justified by the random phase approximation (RPA) of de Gennes [39], could model scattering at all

concentrations and angles [40-42]. This approach is limited to Gaussian, linear chains $\left(d_f = 2\right)$ since it utilizes equation (1), so it does not address the issues of chain topology or excluded volume.

Inter-arm correlations lead to steric straightening of the arms, lowering d_f, in direct analogy to surface grafted chains and polymer brushes. It is desirable to quantify these steric interactions in order to understand the structure of complex macromolecular topologies. This paper derives and applies a new scattering function that can account for topological and solvation effects in linear and further, in symmetric star polymers in order to advance the understanding of polymer chain structure, particularly in solution.

Scaling Model for Symmetric Star Polymers

Complex macromolecules and fractal aggregates can be described in terms of two distinct structural features, the topology and the tortuosity. The structural topology is the structure in the absence of convolution or tortuosity, with the molecule straightened out. For example a linear chain or an H-polymer. The topology is determined at the time of synthesis and can only be changed by breaking bonds. A linear chain in extended conformation, theta, collapsed, or good solvent conditions has the same topology. Tortuosity reflects the convolution of the structure. Therefore the solvent goodness and steric constraints have an impact on the molecular tortuosity but not on the molecular topology. The topology as well as tortuosity of an object must be simultaneously determined in order to reconstruct an average picture of that object. Topology is reflected in the connectivity dimension, *c*, and tortuosity in the minimum dimension, d_{min}, as

described in figure 1, just as the overall structure is described by the mass fractal dimension, d_f.

Beaucage described a scaling model for branched polymers [37] considering a macromolecular chain composed of z Kuhn units of length l_k [43]. Figure 1 shows a 4-arm symmetric star. The structure displays tortuosity in the chain path through the arms, controlled by thermal fluctuations, chain continuity and steric constraints. The scaling model considers the average minimum path of p Kuhn units from one end to another, through the structure, as shown in dark units in figure 1 [37, 44, 45]. A minimum path is the path an electric current would follow through the structure undergoing minimum possible distance to cross the structure. There are $f(f-1)/2$ possible minimum paths to cross the structure through a star with a functionality of f. One of the possible minimum paths is shown in bold in figure 1, where $f = 4$. An average connectivity path of s Kuhn units composed of straight lines connecting the branch point and chain end-points is shown by dashed straight lines in figure 1.

For symmetric star polymers, the minimum path, p, is composed of two arms (dark units in figure 1),

$$p = 2\left(\frac{z}{f}\right) \tag{2}$$

The minimum path, p, is related to the mass, z, through the connectivity dimension, c, while the connectivity path, s, is related to the mass through the minimum dimension, $d_{\min}$, the mass fractal dimension for the minimum path [37],

$$z = p^c = s^{d_{\min}} \tag{3}$$

The connectivity dimension, c is related to the fractal dimension, d_f as [37],

$$d_f = cd_{\min} \tag{4}$$

c increases with increased branching while $d_{\min}$ increases with tortuosity of the chain. For a linear polymer chain, $d_{\min} = d_f$ and c = 1 while, for a completely connected regular object like a sphere or a collapsed coil, and $d_f = c$, since the minimum path (or short circuit path) is a straight line through any regular object (rod, disk, or sphere). For a chain in a θ-solvent, with no steric constraint, $d_{\min} = 2$, while for a similar chain in good solvent, $d_{\min} = 5/3$ [37].

For symmetric stars, the mole fraction branch content (ϕ_{br}) is given by [37],

$$\phi_{br} = \frac{z-p}{z} = 1 - z^{\frac{1}{c}-1} = \frac{f-2}{f} \tag{5}$$

where, $(z-p)$ represents the mass of the coil that does not lie on the minimum path. For a four arm star, $\phi_{br} = 0.5$. Further, the connectivity dimension, c, may be calculated for symmetric stars from equation (5) as,

$$c = \frac{\ln z}{\left[\ln z + \ln\left(\frac{2}{f}\right)\right]} \tag{6}$$

From (5), at high molecular weights, a star polymer approaches the connectivity of a linear chain since $c \to 1$ as the branch site is diluted. (The radius of gyration distinguishes linear from branched structures in this case). A "meandering" mole fraction (ϕ_m) accounts for mass that is not used in direct or ballistic connectivity,

$$\phi_m = \frac{z-s}{z} = 1 - z^{\frac{1}{d_{\min}}-1} \tag{7}$$

As the functionality, *f*, increases, $d_{\min}$ and ϕ_m are expected to decrease since steric constraints on the chain increase. For linear chains $(c=1; f=2)$. In the absence of steric affects, good solvent scaling behavior is expected, $d_{\min}=5/3$, except at the θ-point where $d_{\min}=2$. Steric interactions extend the star arms towards, $d_{\min}\to 1$, for a fully sterically-extended arm. We can use these limits to define a measure of steric interaction between the arms of a star,

$$\phi_{si}=\frac{s_{observed}-s_{unperturbed}}{s_{extended}-s_{unperturbed}}=\frac{z^{\frac{1}{d_{\min}}}-z^{\frac{1}{d_{f,l}}}}{z-z^{\frac{1}{d_{f,l}}}} \tag{8}$$

where $d_{f,l}$ is the fractal dimension of an unperturbed arm under the given solvation conditions [26]. $d_{f,l}$ = 5/3, 2 or 3 under good-solvent, θ-solvent or collapsed conformations respectively. ϕ_{si} is the first quantitative measure of steric effects in stars (extendible to any branched structure). Mathematically, ϕ_{si} gives a measure of the observed extension of branched coil from that of its linear counterpart normalized by its maximum extension. ϕ_{si} is zero for a linear polymer (minimum intra-coil steric hindrances) and attains a maximum value of 1 for a star with rigid straight chains.

Small-Angle Neutron Scattering

Small-angle scattering can be used to quantify the scaling model parameters as previously reported by Beaucage [37]. The enthalpy of mixing for a polymer in solution can be described using the RPA equation [40, 46, 47],

$$\frac{k_n}{I(q)}=\left[\sum_i \frac{1}{v_i z_i \phi_i g(q)}-\frac{2\chi}{v_0}\right] \tag{9}$$

where the summation runs over all of the solution components including the solvent. z is the weight average number of Kuhn units in the polymer, ϕ is the polymer volume fraction, $g(q)$ is the chain form factor in the absence of enthalpic interactions $(\chi = 0)$, χ is the Flory-Huggins's enthalpic interaction parameter (empirical) [47] and v_0 is the average segmental volume [48],

$$\upsilon_0 = \left(v_{pol} v_{sol}\right)^{1/2} = \left[\left(\frac{M_{w,Kuhn}}{\rho_{Kuhn}}\right)\left(\frac{M_{solv}}{\rho_{solv}}\right)\right]^{1/2} \tag{10}$$

where, v_{pol} and v_{sol} are the segmental volume of the Kuhn unit and the solvent molecule respectively. The scattering constant k_n, which is proportional to scattering contrast, is [3, 46],

$$k_n = N_A\left(b_{pol} - b_{sol}\right)^2 \tag{11}$$

where, N_A is the Avogadro's number, and b_{pol} and b_{sol} are the scattering length densities of polymer Kuhn unit and solvent molecule respectively.

Coupling equation (9) with the Unified Function for branched structures [37], a hybrid scattering function that accounts for branching and enthalpic screening is obtained,

$$\frac{1}{I(q)} = \frac{1}{G_f}\left\{\left[\left\{e^{-\left(q^2 R_{g,f}^2\right)/3} + K_f e^{-\left(q^2 l_p^2\right)/9}\left(q_f^*\right)^{-d_f}\right\} + \frac{1}{z}\left\{e^{-\left(q^2 l_p^2\right)/9} + zK_p\left(q_p^*\right)^{-1}\right\}\right]^{-1} + z\phi K_v\left(1 - \frac{2\chi}{\sqrt{K_v}}\right)\right\} \tag{12}$$

where, $K_v = \frac{v_{pol}}{v_{sol}}$, $q_i^* = q\Big/\left\{erf\left(qk_{sc}R_{g,i}/\sqrt{6}\right)\right\}^3$, $k_{sc} \approx 1.06$, and *erf* is the error function [49, 50]. The terms in the first curved bracket with subscript, *f*, represent the fractal scaling regime, and the second bracket with subscript, *p*, represent the rod-like persistent scaling

regime. K_f and K_p are ratios of power-law prefactor to Guinier prefactor for fractal and persistent regimes respectively. $R_{g,f}$ is the radius of gyration for the fractal structures. The Guinier prefactor for the fractal regime is given by,

$$G_f = v_{pol} z \phi N_A \left(b_{pol} - b_{sol} \right)^2 \tag{13}$$

and,

$$z = G_f / G_p \tag{14}$$

where, z is the weight average number of Kuhn units in the whole structure [37]. Inclusion of the interaction parameter in equation (12) can play a large part in determining the scattering curve, especially at low-q, at high concentration and where $\chi / \sqrt{K_v}$ << 0.5. Equation (12) fails to account for correlations between arms in a symmetric star polymer, so it is applicable only to disordered branched structures with a functionality of ~3 such as long-chain branched, high-density polyethylene in good solvents.

The chain form factor in equation (12) is based on the Unified Function proposed by Beaucage which is widely utilized to quantify fractal systems [37, 51]. For branched systems the scattering function is obtained by an extrapolation of an integral form proposed by Benoit to the high-q power-law regime and to the $I(0) = G$ intercept. These extrapolations are substituted for G_f and B_f in the Unified Function. The integral form for topologically complex structures is obtained from [52, 53],

$$\frac{I(q)}{G} = \left(\frac{2}{p^2} \right) p^{1-c} \int_0^p n^{c-1} \left(p - n \right) e^{-q^2 R_{g,n}^2} \, dn \tag{15}$$

In reference [37] the integration in equation (15) is over the minimum path, *p via* minimum path index, *n*, which goes from *0* to *p* [37, 49, 50]. By substitution of parameters Beaucage obtains [37, 51],

$$\frac{I(q)}{G} = \frac{d_{\min}}{\left(qR_g\right)^{d_f}} \int_0^{\left(qR_g\right)^2} \left[1 - \frac{y^{\frac{d_{\min}}{2}}}{\left(qR_g\right)^{d_{\min}}}\right] e^{-y} y^{\left(\frac{d_f}{2}-1\right)} dy \tag{16}$$

As noted by Beaucage [37], equation (15) ignores correlations between chain segments that are not linearly bonded. To account for correlations between topologically connected chains, like binary inter-arm interactions in star polymers, the approach proposed by Benoit and later Alessandrini for symmetric star polymers can be employed [32, 54]. For interaction amongst arms of an *f*-arm, symmetric star polymer, equation (15) is expanded to include the inter-arm interactions following Benoit and Alessandrini [32, 54],

$$\frac{I(q)}{G} = \left[\begin{array}{l} \binom{f}{1}\left(\frac{2}{p^2}\right) p^{1-c} \int_0^p i^{c-1}\left(p-i\right) e^{-q^2 R_{g,i}^2}\, di \\ + \binom{f}{2}\left(\frac{2}{p^2}\right)^2 p^{2(1-c)} \int_0^p j^{c-1}\left(p-j\right) e^{-q^2 R_{g,j}^2}\, dj \int_0^p k^{c-1}\left(p-k\right) e^{-q^2 R_{g,k}^2}\, dk \end{array}\right] \tag{17}$$

where, the interaction integrals are over $\binom{f}{1} = \frac{f!}{n!(f-n)!}$ pair of arms. Substituting for variables, similar to Beaucage and Benoit [32, 37],

$$i = \left(\frac{6R_{g,i}^2}{R_1^2}\right)^{\frac{d_{\min}}{2}} = \frac{1}{q^{d_{\min}}}\left(\frac{6u}{R_1^2}\right)^{\frac{d_{\min}}{2}} \Rightarrow di = \frac{6}{R_1^2}\frac{1}{q^{d_{\min}}}\frac{d_{\min}}{2}\left(\frac{6u}{R_1^2}\right)^{\frac{d_{\min}}{2}-1} du \tag{18}$$

$$j = \left(\frac{6R_{g,j}^2}{R_1^2}\right)^{\frac{d_{\min}}{2}} = \frac{1}{q^{d_{\min}}}\left(\frac{6v}{R_1^2}\right)^{\frac{d_{\min}}{2}} \Rightarrow dj = \frac{6}{R_1^2}\frac{1}{q^{d_{\min}}}\frac{d_{\min}}{2}\left(\frac{6v}{R_1^2}\right)^{\frac{d_{\min}}{2}-1} dv \tag{18'}$$

$$k = \left(\frac{6R_{g,k}^2}{R_1^2}\right)^{\frac{d_{\min}}{2}} = \frac{1}{q^{d_{\min}}}\left(\frac{6w}{R_1^2}\right)^{\frac{d_{\min}}{2}} \Rightarrow dk = \frac{6}{R_1^2}\frac{1}{q^{d_{\min}}}\frac{d_{\min}}{2}\left(\frac{6w}{R_1^2}\right)^{\frac{d_{\min}}{2}-1} dw \tag{18"}$$

$$p = \left(\frac{6R_g^2}{R_1^2}\right)^{\frac{d_{\min}}{2}} \tag{19}$$

in equation (17) yields,

$$\frac{I(q)}{G} = \left[\begin{array}{l} f\dfrac{d_{\min}}{\left(qR_g\right)^{d_f}}\displaystyle\int_0^{\left(qR_g\right)^2}\left[1-\frac{u^{\frac{d_{\min}}{2}}}{\left(qR_g\right)^{d_{\min}}}\right]e^{-u}u^{\left(\frac{d_f}{2}-1\right)}du \\ +\dfrac{f(f-1)}{2}\dfrac{d_{\min}^2}{\left(qR_g\right)^{2d_f}}\displaystyle\int_0^{\left(qR_g\right)^2}\int_0^{\left(qR_g\right)^2}\left[1-\frac{v^{\frac{d_{\min}}{2}}}{\left(qR_g\right)^{d_{\min}}}\right]\left[1-\frac{w^{\frac{d_{\min}}{2}}}{\left(qR_g\right)^{d_{\min}}}\right]e^{-(v+w)}(vw)^{\left(\frac{d_f}{2}-1\right)}dv\,dw \end{array}\right] \tag{20}$$

Equation (20) has two structural levels, the first corresponding to arm scattering and the second to binary arm correlations. The exponents outside the single and double integrals, in the first and second terms of equation (20), respectively, constitute the $I(0)$ prefactors for the arm scattering term, G_f, and the binary arm correlation term, G_{2f}. G_f is simply the prefactor for a single arm times the number of arms, *f*,

$$G_f = fG \tag{21}$$

and G_{2f} is given by,

$$G_{2f} = \left[\frac{f(f-1)}{2}\right]G = \left[\frac{f-1}{2}\right]G_f \tag{22}$$

For the power law pre-factor in the Unified function, B, the asymptotes are [37, 51],

$$B_f = \frac{G_f d_{\min}\Gamma\left(\frac{d_f}{2}\right)}{R_g^{d_f}} \tag{23}$$

$$B_{2f} = \frac{G_{2f} d_{\min}^2 \Gamma\left(d_f - 1\right)}{R_g^{2d_f}} = \frac{\left(f-1\right) G_f d_{\min}^2 \Gamma\left(d_f - 1\right)}{2R_g^{2d_f}} \tag{24}$$

From equation (23), $d_{\min}$ is given by [37, 44, 55],

$$d_{\min} = \frac{B_f R_g^{d_f}}{G_f \Gamma\left(\frac{d_f}{2}\right)} \tag{25}$$

where, Γ is the gamma function. Equation (25) is valid for monodisperse samples [44, 55]. From d_f and $d_{\min}$, c can be obtained using equation (4) and p and s, using equations (2) and (3).

With these substitutions equation (12) becomes,

$$\frac{1}{I(q)} = \frac{1}{G_f}\left\{\left[\begin{array}{l} \dfrac{f-1}{2}\left\{e^{-\left(q^2 R_g^2\right)/3} + \dfrac{d_{\min}^2 \Gamma\left(d_f - 1\right)}{R_g^{2d_f}} e^{-\left(q^2 l_p^2\right)/9} \left(q_f^*\right)^{-2d_f}\right\} \\ + \left\{e^{-\left(q^2 R_g^2\right)/3} + K_f e^{-\left(q^2 l_p^2\right)/9} \left(q_f^*\right)^{-d_f}\right\} + \dfrac{1}{z}\left\{e^{-\left(q^2 l_p^2\right)/9} + zK_p\left(q_p^*\right)^{-1}\right\} \end{array}\right]^{-1} + z\phi K_v\left(1 - \frac{2\chi}{\sqrt{K_v}}\right)\right\} \tag{26}$$

The first term, with the lead factor $\left(f-1\right)/2$, accounts for binary correlations between the arms. This term has a steep power law slope of $-2d_f$. In the original Benoit expression this term has a slope of -4 and accounts for a steep upturn in the scattering at low-q. The second term is similar to equation (12) and reflects scattering from the arms in the absence of correlations between arms. This term includes a structural level describing chain persistence. The final term accounts for screening due to enthalpic interactions, serving to diminish the intensity at low-q under good solvent conditions at high

concentrations. Under the condition that $f = 1$ for a linear chain, equation (26) reverts to equation (12) [21, 32, 41, 54, 56].

The evaluated χ parameter is per Kuhn unit, similar to *z*, and not per mer unit, which means that the χ values evaluated using equation (26) above are based on zero conformational entropy units versus the traditional chemical mer unit. The calculation of χ per unit Kuhn length is therefore thermodynamically more relevant but may not be directly compared to values reported in literature, as the structural basis is different. Nevertheless, the second virial coefficient (A_2) may be alternately used to alleviate the issues with base structure. A_2 is given by,

$$A_2 = \frac{\left(\frac{1}{2} - \chi\right)}{V_{sol}\rho_{pol}^2} \tag{27}$$

where, V_{sol} is the molar volume of the solvent (evaluated to be 123.3 cm^3/mol for *p*-xylene) and ρ_{pol} is the density of polymer (~0.916 g/cm^3 for polyisoprene).

For the polymer/solvent system under present consideration, and perhaps more generally, the initial hint of a transition from polymeric/fractal structure to a colloidal, Daoud Cotton structure may begin near $f > 8$. For different systems this cutoff may occur at different functionalities but $f > 8$ as a rule of thumb would be presently suggested for appearance of colloidal features. The appearance of a 3D core is considered as a sign of colloidal structure for the star polymers. This transition point with increasing *f* is a limit to the applicability of the proposed scattering function.

Material and Method

Linear and 4 and 8 arm symmetric star polyisoprene samples were used. The Linear standard was purchased from PSS Polymer Standards Service GmbH, Mainz, Germany with M_w of 110kg/mole, M_n of 109kg/mole, and PDI of 1.01. The 4-arm and 8-arm polyisoprene stars were synthesized by anionic polymerization using high vacuum techniques and chlorosilane chemistry [57]. All intermediate and final products were analyzed by size exclusion chromatography (SEC) and nuclear magnetic resonance spectroscopy. The molecular weight of the arms (by SEC) and final star polymers (by SEC-MALLS) are given in table I.

SANS was performed on dilute solutions of model star isoprene in deuterated *p*-xylene at 34.5° C. 500 ppm of butylhydroxytoluene (BHT) was added to as a stabilizer. Deuterated p-xylene was purchased from Cambridge Isotopes. The PI samples were equilibrated at 34.5°C for 2 hours prior to the measurements to ensure complete dissolution of the polymer in solvent. One weight percent solutions were used, which is below the overlap concentration. SANS experiments were carried out at HFIR CG-2 General-Purpose SANS facility at the Oak Ridge National Laboratory (ORNL) and at NCNR NG7 SANS facility at the National Institute of Standards and Technology (NIST). At CG-2 HFIR, SANS experiments were run at sample to detector distances of 18.5m and 0.75m, while at NG7 NCNR, experiments were done at 15, 7 and 1m. The low-*q* data was calibrated with standards to obtain absolute intensity.

Results and Discussion

Figure 2(a) shows SANS data from a ~1% solution by weight of the linear standard, 4-arm and 8-arm polyisoprene symmetric star polymers in *d*-xylene solvent.

The overlapping scattering curves clearly show deviations at low-q [42]. The Unified Fit for the 4-arm polyisoprene symmetric star polymer in figure 2(b) shows two structural levels for the mass-fractal, at intermediate-q, the fractal-scaling regime, and at high-q, the persistence regime. The SANS data fits from linear, 4-arm and 8-arm polyisoprene using the hybrid Unified Function, equation (26), is shown in figure 2(c) with offsets for visual clarifications.

The inter-arm interaction scattering in grey dashed lines in figure 2(b) that decays faster in lower-q regime, comes from the first term, with the lead factor $(f-1)/2$, in equation (26) which accounts for binary correlations between the arms. The fractal scattering comes from scattering from the chain arms in the absence of correlations between arms and has two sets of parameters for the fractal and persistence scattering regimes [44]. These two sets of fitting curves then add up, as shown in grey dash-dot-dots, and are screened at low-q by the inverse of the χ term in equation (26) shown as grey dash-dots in Figure 2(b).

The fitted and calculated scaling and thermodynamic parameters are listed in table II. The interaction parameter for the samples varied from 0.34±0.02 to 0.22±0.03 and 0.31±0.01 for the linear, 4-arm, and 8-arm stars respectively, which compare rather well with the reported values for χ to be 0.27 [58, 59]. It is to be noted that the fitted values of empirical parameter, χ is per unit Kuhn length, which is the smallest zero conformational entropy unit of the polymer chain, as pointed out earlier. The second virial coefficient for the linear, 4-arm and 8-arm star polymers were estimated to be 0.0015±0.0002, 0.0027±0.0003 and 0.0018±0.0001 molcm^3/g^2. The persistence lengths

for the three samples were evaluated to be 13.2±0.1 Å, 13.6±0.3 Å and 12.6±0.3 Å. Neither of the two parameters, χ/A_2 or l_p, demonstrated any clear relation to the functionality of the star polymers. The mass fractal dimension is close to 5/3 as expected from figure 2(a).

The respective minimum paths, p, of 145±2, 130±1 and 126±1 for the three samples in Kuhn units remained within ~10% of each other while the respective minimum dimensions of 1.72±0.09, 1.46±0.06 and 1.43±0.05, reflected increase in stretching of the arms in space with number of arms as compared to a linear chain under good solvent conditions. The connective paths, s, of 18±3, 45±7 and 115±21 Kuhn units, displayed a connectivity dimensions, c, of 1.00±0.09, 1.14±0.08 and 1.29±0.07 which reflects increase in branching and connectivity in the star polymers with functionality. The branch fraction, ϕ_{br}, which was calculated by equation (5) and bound by equation (6), was determined to be 0, 0.50±0.06 and 0.75±0.21 for linear, 4-arm and 8-arm symmetric stars following the expected value from, $(f-2)/f$. The meandering fraction, ϕ_m, which is the fraction of excess mass due to tortuosity in the system, was calculated to be 0.88±0.14, 0.83±0.13 and 0.77±0.14 for the respective samples using equation (7) which indicated that the arms stretch in space with increasing functionality and hence a larger number of structural Kuhn units, z, are necessary to connect the branch point to the free end, as functionality increases.

The steric interaction fraction, ϕ_{si}, is an important quantification of the steric interactions of arms compared to the maximum possible steric interaction. It is 0 for an unbranched polymer chain and is expected to increase with increasing functionality. ϕ_{si} is calculated to be ~0, 0.08±0.05, 0.17±0.07 for the linear, 4-arm and 8-arm samples

respectively. This value reflects an increasing steric interaction with increase in functionality in symmetric star polymers.

Conclusions

The effect of molecular weight and functionality is of great significance to exploitation of the properties of star polymers, which can acquire a wide range of conformations under varying structural and thermodynamic constraints. A versatile method to characterize such structures greatly enhances the capability to establish robust structure-property relationships. A scaling model for symmetric star polymers was presented and a method to utilize SANS to obtain scaling parameters was demonstrated. The scaling approach is expected to better describe these systems under different solvation conditions than previous methods because it can accommodate and distinguish changes in topology, tortuosity, and thermodynamics.

A scattering function was derived which takes account of the inter-arm correlations and the polymer-solvent interaction parameter. The concept of branch fraction, ϕ_{br}, was used for quantification of star functionality since it can be directly obtained by analysis of scattering data using the scaling approach. The approach was successfully applied to linear, 4-arm and 8-arm PI stars and the results were discussed. This versatile method to quantify the structural as well as thermodynamic parameters should greatly enhance capabilities to establish robust structure-property relationships for such systems.

Acknowledgements

The research conducted at ORNL's High Flux Isotope Reactor was sponsored by the Scientific User Facilities Division, Office of Basic Energy Sciences, US Department

of Energy. We acknowledge the support of the National Institute of Standards and Technology, U.S. Department of Commerce, in providing the neutron research facilities used in this work.

References

1 B. H. Zimm and W. H. Stockmayer, The Journal of Chemical Physics **17**, 1301 (1949).

2 G. Widawski, M. Rawiso, and B. Francois, Nature **369**, 387 (1994).

3 G. S. Grest, L. J. Fetters, J. S. Huang, and D. Richter, Advances in Chemical Physics, Vol Xciv **94**, 67 (1996).

4 S. T. Milner and T. C. B. McLeish, Macromolecules **31**, 7479 (1998).

5 M. Watzlawek, C. N. Likos, and H. Lowen, Physical Review Letters **82**, 5289 (1999).

6 N. Hadjichristidis, M. Pitsikalis, S. Pispas, and H. Iatrou, Chemical Reviews **101** 3747 (2001).

7 P. G. De Gennes, *Scaling Concepts in Polymer Physics* (Cornell University Press, New York, 1979).

8 B. Capone, I. Coluzza, F. LoVerso, C. N. Likos, and R. Blaak, Physical Review Letters **109** 238301 (2012).

9 M. Ripoll, R. G. Winkler, and G. Gompper, Physical Review Letters **96** 188302 (2006).

10 M. Daoud and J. P. Cotton, Journal De Physique **43**, 531 (1982).

11 T. M. Birshtein and E. B. Zhulina, Polymer **25**, 1453 (1984).

12 J. Batoulis and K. Kremer, Macromolecules **22**, 4277 (1989).

13 W. D. Dozier, J. S. Huang, and L. J. Fetters, Macromolecules **24**, 2810 (1991).

14 J. Roovers, P. M. Toporowski, and J. Douglas, Macromolecules **28**, 7064 (1995).

15 C. Picot, F. Audouin, and C. Mathis, Macromolecules **40**, 1643 (2007).

16 F. Lo Verso, C. N. Likos, C. Mayer, and H. Lowen, Physical Review Letters **96** 187802 (2006).

17 S. V. Panyukov, S. S. Sheiko, and M. Rubinstein, Physical Review Letters **102** 148301 (2009).

18 E. Glynos, B. Frieberg, and P. F. Green, Physical Review Letters **107** 118303 (2011).

19 A. Jusufi, C. N. Likos, and H. Lowen, Physical Review Letters **88** 018301 (2001).

20 C. N. Likos, H. Lowen, M. Watzlawek, B. Abbas, O. Jucknischke, J. Allgaier, and D. Richter, Physical Review Letters **80**, 4450 (1998).

21 J. C. Horton, G. L. Squires, A. T. Boothroyd, L. J. Fetters, A. R. Rennie, C. J. Glinka, and R. A. Robinson, Macromolecules **22**, 681 (1989).

22 L. J. Fetters, A. D. Kiss, D. S. Pearson, G. F. Quack, and F. J. Vitus, Macromolecules **26** 647 (1993).

23 L. Willner, O. Jucknischke, D. Richter, J. Roovers, L. L. Zhou, P. M. Toporowski, L. J. Fetters, J. S. Huang, M. Y. Lin, and N. Hadjichristidis, Macromolecules **27**, 3821 (1994).

24 P. M. Wood-Adams, J. M. Dealy, A. W. deGroot, and O. D. Redwine, Macromolecules **33** 7489 (2000).

25 A. I. Norman, D. L. Ho, and S. C. Greer, Macromolecules **40**, 9628 (2007).

26 R. Ramachandran, G. Beaucage, D. K. Rai, D. J. Lohse, T. Sun, A. H. Tsou, A. Norman, and N. Hadjichristidis, Macromolecules **45**, 1056 (2012).

27 T. Niitani, M. Amaike, H. Nakano, K. Dokko, and K. Kanamura, Journal of the Electrochemical Society **156**, A577 (2009).

28 W. H. Shih, W. Y. Shih, S. I. Kim, J. Liu, and I. A. Aksay, Physical Review A **42**, 4772 (1990).

29 L. Y. Qiu and Y. H. Bae, Pharmaceutical Research **23**, 1 (2006).

30 H. Wei, X. Zhang, C. Cheng, S. X. Cheng, and R.-X. Zhuo, Biomaterials **28**, 99 (2007).

31 W. Jakubowski, P. McCarthy, N. Tsarevsky, and J. Spanswick, in *US Patent, US 8173750 B2* (ATRP Solutions, Inc. Pittsburgh, PA, United States, 2012), Vol. 8173750.

32 H. Benoit, J. Polym. Sci. **11**, 507 (1953).

33 J. S. Higgins and H. C. Benoit, *Polymers and Neutron Scattering* (Oxford science Publications, Oxford, 1994).

34 J. S. Pedersen, Advances in Colloid and Interface Science **70**, 171 (1997).

35 X. Li, C. Do, Y. Liu, L. Sanchez-Diaz, G. Smith, and W.-R. Chen, Journal of Applied Crystallography **47**, 1901 (2014).

36 U. S. Jeng, T. L. Lin, L. Y. Wang, L. Y. Chiang, D. L. Ho, and C. C. Han, Appl. Phys. A-Mater. Sci. Process. **74**, S487 (2002).

37 G. Beaucage, Physical Review E **70**, 031401 (2004).

38 R. S. Stein and G. Hadziioannou, Macromolecules **17**, 1059 (1984).

39 G. Strobl, *The Physics of Polymers: Concepts for Understanding Their Structures and Behavior* (Springer, New York, 2007).

40 J. Stellbrink, L. Willner, O. Jucknischke, D. Richter, P. Lindner, L. J. Fetters, and J. S. Huang, Macromolecules **31**, 4189 (1998).

41 J. Stellbrink, L. Willner, D. Richter, P. Lindner, L. J. Fetters, and J. S. Huang, Macromolecules **32**, 5321 (1999).

42 J. Stellbrink, et al., Applied Physics a-Materials Science & Processing **74**, S355 (2002).

43 W. Kuhn, Kolloid-Zeitschrift **68**, 2 (1934).

44 R. Ramachandran, G. Beaucage, A. S. Kulkarni, D. McFaddin, J. Merrick-Mack, and V. Galiatsatos, Macromolecules **41**, 9802 (2008).

45 G. Beaucage and A. S. Kulkarni, Macromolecules **43**, 532 (2010).

46 G. Beaucage and R. S. Stein, Macromolecules **26**, 1617 (1993).

47 A. Zirkel, S. M. Gruner, V. Urban, and P. Thiyagarajan, Macromolecules **35**, 7375 (2002).

48 J. F. Joanny, Comptes Rendus Hebdomadaires Des Seances De L Academie Des Sciences Serie B **286**, 89 (1978).

49 G. Beaucage, Journal of Applied Crystallography **28**, 717 (1995).

50 G. Beaucage, Journal of Applied Crystallography **29**, 134 (1996).

51 H. Benoit, Hebd. Seances Acad. Sci. **245**, 2244 (1957).

52 P. Debye, Journal of Physical and Colloid Chemistry **51**, 18 (1947).

53 A. Peterlin, Makromol. Chem. **9**, 244 (1953).

54 J. L. Alessandrini and M. A. Carignano, Macromolecules **25**, 1157 (1992).

55 R. Ramachandran, G. Beaucage, A. S. Kulkarni, D. McFaddin, J. Merrick-Mack, and V. Galiatsatos, Macromolecules **42**, 4746 (2009).

56 W. H. Stockmayer and M. Fixman, Annals of the New York Academy of Sciences **57**, 19 (1953).

57 N. Hadjichristidis, H. Iatrou, S. Pispas, and M. Pitsikalis, Journal of Polymer Science Part a-Polymer Chemistry **38**, 3211 (2000).

58 Y. B. Tewari and H. P. Schreiber, Macromolecules **5**, 329 (1972).

59 J. E. Mark, *Physical Properties of Polymers* (Cambridge University Press, 2004).

Figures

FIG. 1: Schematic of a four arm PI star polymer in 2-D. Four PI arms are connected to a tetrafunctional Si atom forming the 4-arm PI star with mass, z, fractal dimension, d_f, and connective dimension, c. A minimum path, p, with a dimension, $d_{\min}$, which describes molecular tortuosity, is shown in dark units. The connective path, composed of s units, is shown by dashed straight lines. Scaling features are described in the text.

FIG. 2 (a) SANS from solution of ~1% by weight linear standard, 4-arm star and 8-arm star polyisoprene in xylene solvent in light grey dots, dark grey dashes and solid black line. The slope of 5/3 and 1 are also shown. (b) SANS from 4-arm polyisoprene in grey circles with the final Hybrid Unified Fit [equation (26)] in black line. The contribution from fractal chain scattering, the inter-arm interaction, their sum and χ-term are also presented. Please note the deviation of chain scattering from the Unified Fit near the Guinier knee. (c) SANS from linear, 4-arm and 8-arm polyisoprene with Hybrid Unified Fits with offsets for visual clarifications. The low-q correlation features are present due to the inter-correlation amongst the arms in the star as the concentration of 1wt% was below the overlap concentration.

Tables

Table I. Synthesis and characterization details for linear, 4-arm and 8-arm PI star polymers.

Table II. Fitted, thermodynamic and calculated scaling parameters for PI polymer samples using the Unified equation (26)

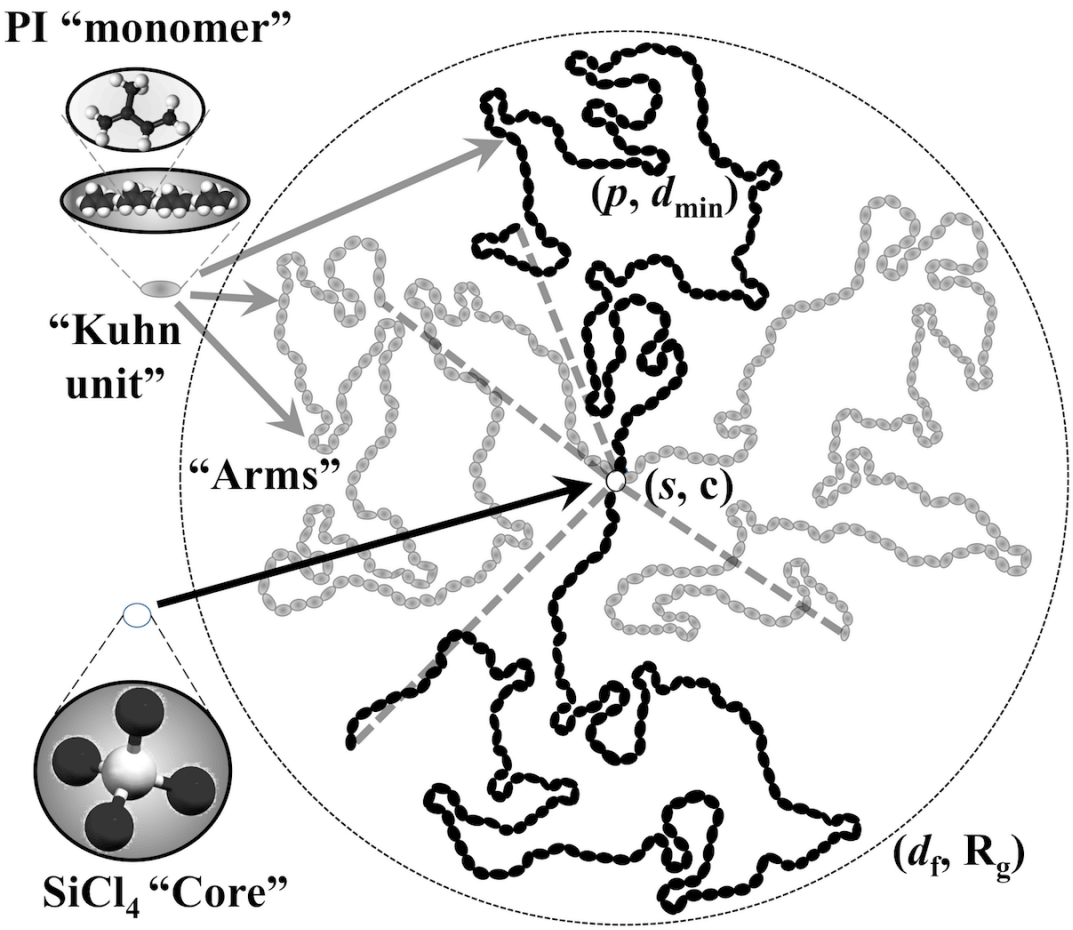

Figure 1

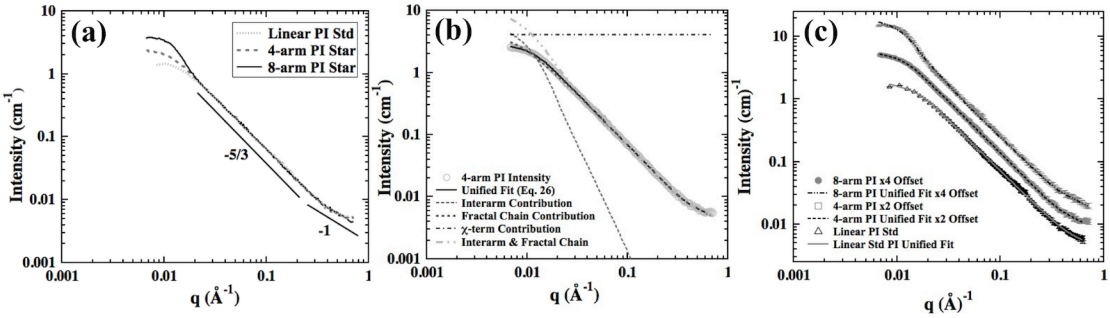
(a)
Linear PI Std
4-arm PI Star
8-arm PI Star
-5/3
-1
Intensity (cm^{-1})
q (Å^{-1})
(b)
4-arm PI Intensity
Unified Fit (Eq. 26)
Interarm Contribution
Fractal Chain Contribution
χ-term Contribution
Interarm & Fractal Chain
Intensity (cm^{-1})
q (Å^{-1})
(c)
8-arm PI x4 Offset
8-arm PI Unified Fit x4 Offset
4-arm PI x2 Offset
4-arm PI Unified Fit x2 Offset
Linear PI Std
Linear Std PI Unified Fit
Intensity (cm)$^{-1}$
q (Å)$^{-1}$

Figure 2

1,4-PI	M_n arm (kg/mol), SEC			Final star-branched PI (SEC-MALS)		f = $M_{n,star}/M_{n,arm}$	
	Cal.[a]	*SEC*[b]	M_w/M_n	M_n, kg/mol	M_w/M_n	*Cal.*[a]	*SEC*[b]
Linear*	*110*	*1.01**	-	-	*1*	*Linear**	*110*
4-arm star	*61*	*55*	*1.01*	*218.9*	*1.01*	*3.59*	*3.98*
8-arm star	*60*	*55*	*1.01*	*415.4*	*1.01*	*6.92*	*7.55*

**Purchased from PSS Polymer Standards Service GmbH (Mw of 110 kg/mole, Mn of 109 kg/mole),* [a] *Calculated values from chemical stoichiometry,* [b] *SEC/MALS determined values.*

Table 1

Sample	R_g (Å)	z	d_f	χ^*	$A_2 \times 10^3$ ($molcm^3 g^{-2}$)	l_p (Å)	d_{min}	c	p	s	ϕ_{br}	ϕ_m	ϕ_{si}
Linear Std	*130 ±2*	*145 ±2*	*1.72 ±0.06*	*0.34 ±0.02*	*1.5 ±0.2*	*13.2 ±0.1*	*1.72 ±0.09*	*1.00 ±0.09*	*145 ±2*	*18 ±3*	*0.0 ±0.0*	*0.88 ±0.14*	*0.0 ±0.0*
4-arm	*165 ±7*	*260 ±3*	*1.67 ±0.04*	*0.22 ±0.03*	*2.7 ±0.3*	*13.6 ±0.3*	*1.46 ±0.06*	*1.14 ±0.08*	*130 ±1*	*45 ±7*	*0.50 ±0.17*	*0.83 ±0.13*	*0.08 ±0.05*
8-arm	*224 ±3*	*503 ±7*	*1.69 ±0.03*	*0.31 ±0.01*	*1.8 ±0.1*	*12.6 ±0.3*	*1.43 ±0.05*	*1.29 ±0.07*	*126 ±1*	*115 ±21*	*0.75 ±0.21*	*0.77 ±0.14*	*0.17 ±0.07*

* χ determined per Kuhn unit.

Table 2